Dynamical Description of Transient X-Ray Lasers Seeded with High-Order Harmonic Radiation through Maxwell-Bloch Numerical Simulations

I. R. Al'miev,[1] O. Larroche,[2,*] D. Benredjem,[1] J. Dubau,[1] S. Kazamias,[1] C. Möller,[1] and A. Klisnick[1]

[1]*LIXAM, Bâtiment 350, Université Paris-Sud, 91405 Orsay Cedex, France*

[2]*CEA-DIF, BP 12, 91680 Bruyères le Châtel, France*

(Received 11 June 2007; published 21 September 2007)

The Maxwell-Bloch code COLAX has been upgraded to use detailed hydrodynamical and collisional-radiative simulations of a soft x-ray laser plasma with traveling-wave pumping. The seeding of short pulses of high-order harmonics of the pump laser into the x-ray laser medium has been simulated. The amplification is shown to be a dynamic, two-stage process: the atomic dipoles of the lasing ions are first coherently excited by the short pulse, and subsequently generate a radiation wake which is amplified along its path through the plasma, with consequences on the experimentally recorded spectra.

DOI: 10.1103/PhysRevLett.99.123902 PACS numbers: 42.55.Vc, 42.50.Gy

Considerable progress has been made over the past few years in the development of high-brightness coherent radiation beams in the soft x-ray region, which will open new opportunities in science. The emerging fourth generation synchrotrons, the so-called x-ray free-electron lasers (XFELs), have now demonstrated unprecedented high peak power in the nanometer spectral region [1] with femtosecond temporal resolution and will be used for various applications. However, for the widespread development of these applications there is a need to develop more compact and less expensive sources. Soft x-ray lasers (XRLs) generated through laser amplification in a hot and dense plasma constitute a promising and complementary alternative. Following their first experimental demonstration in 1985 [2] dramatic progress has been made worldwide in the understanding and performance of these sources [3]. The most recently achieved soft XRLs are able to emit extremely bright and monochromatic pulses in the 10–20 nm wavelength range with a peak brightness that compares well with the XFEL performance in a 10^{-5} spectral bandwidth [4].

However, these soft XRL beams which operate in the amplification of spontaneous emission (ASE) regime suffer from a limited spatial coherence [5]. To overcome this limitation, seeding of the soft x-ray plasma amplifier with high-order harmonics (HOH) of a femtosecond optical laser has been investigated. The first experiment was performed by Ditmire *et al.* [6] more than 10 years ago with a gallium plasma amplifier, but the amplification of the harmonic seed was very low. The first major breakthrough was achieved in 2004 by Zeitoun *et al.* [7] who demonstrated the saturated amplification at 32.8 nm of the 25th harmonic of a Ti:sapphire laser in a krypton soft x-ray amplifier pumped from a gaseous target by optical field ionization. In order to extend these results towards shorter wavelengths and higher output energies, seeding of transient soft XRLs generated in plasmas produced from solid targets are best suited because they operate at a higher density and can be easily extrapolated to higher Z elements. Experimental work towards this goal is thus now receiving a growing interest in the soft XRL and HOH communities, and two experimental demonstrations have been recently reported. A weak amplification of a HOH seed in a Mn transient soft x-ray-laser amplifier was achieved by Kawachi *et al.* at 26.9 nm [8]. More recently Wang *et al.* [9] reported the saturated amplification of the 25th harmonic of a Ti:sapphire laser in a Ti soft XRL, operating at a repetition rate of 5 Hz. To support these experimental investigations and because very little is known yet on the fundamental behavior of seeded soft XRLs, detailed numerical modeling is required.

In this Letter we report some theoretical advances in the modeling of these systems. Our goal is to simulate the propagation and amplification of a short HOH pulse within a Ni-like Ag laser-produced plasma created by the traveling-wave (TW) irradiation of a solid target, which creates a strong transient population inversion on the $4d$-$4p$ transition at 13.9 nm. Let us emphasize that, due to its short duration (of the order of 10 fs), the Fourier-limited spectral width of the HOH pulse is typically 100 times as large as that of the XRL gain curve (of the order of 10^{12} s^{-1}). This makes the Maxwell-Bloch code COLAX particularly well suited to modeling that scheme since it works in the time, rather than spectral, domain. The upgrade of COLAX is reported, along with simulation results which will be shown to crucially depend on a correct treatment of the temporal dynamics of the system.

The conditions of the simulations for the transient soft XRL amplifier match the experimental ones reported by Klisnick *et al.* [10]. We assume that the silver target is irradiated by a long (600 ps) prepulse of relatively low intensity (10^{12} W/cm^2), creating a preplasma. Then, it is irradiated by the main TW pumping pulse of larger intensity (10^{15} W/cm^2) but shorter duration (400 fs), creating conditions for a strong population inversion. The time interval between the prepulse and main pulse is 250 ps.

The angle of the traveling wave, which is related to the velocity of TW irradiation (see Ref. [11] for a discussion of TW generation), can be varied in the present version of the code. In the reference calculation described below, we set it at 45° which corresponds to a TW velocity equal to the speed of light in vacuum. To simulate the Ni-like Ag laser-produced plasma we use the 1.5-dimensional code EHYBRID [12] which self-consistently solves the hydrodynamical and rate equations. The parameters of the HOH seed pulse are chosen to fit the typical experimental features currently available with neon at 13.9 nm [13]. The HOH pulse has a Gaussian shape in time and space with a 15 fs temporal width and a 30 μm spatial width, and the peak intensity is 10^9 W/cm^2, leading to an integrated energy of approximately 0.1 nJ. The injection time of the HOH pulse at the entrance of the plasma amplifier is an adjustable parameter in the code. For the reference calculation we set it at 2 ps after the start of the TW irradiation, to match the time of maximum gain. The parameters used for the simulations described below were not chosen to optimize the output of the amplified HOH pulse, but rather to provide detailed insight in the dynamical response of the plasma to the seed pulse.

The code COLAX was first described in [14], where it was used to model the XRL signal buildup in the long (600 ps) pumping pulse regime. The evolution of the linearly polarized z component of the electric field

$$E_z = \mathrm{Re}[E_+(x, y, t)e^{-i\omega(t-y/c)} + E_-(x, y, t)e^{-i\omega(t+y/c)}]$$

is described by Maxwell's equations, restricted to the following paraxial time-envelope form (see Fig. 1 for a schematic of the system geometry and coordinate axes):

$$\frac{2i\omega}{c}\left(\frac{1}{c}\frac{\partial E_\pm}{\partial t} \pm \frac{\partial E_\pm}{\partial y}\right) + \frac{\partial^2 E_\pm}{\partial x^2} = -\frac{\omega^2}{c^2}[(\epsilon - 1)E_\pm + 4\pi P_\pm]. \quad (1)$$

Here E_+ and E_- are the slowly varying complex amplitudes of waves propagating in the forward ($+y$) and reverse ($-y$) directions, respectively, and ω is the XRL line frequency. ϵ is the dielectric constant of free electrons, which accounts for refraction and collisional damping of the XRL waves. Translational symmetry along z is assumed in the code. The other polarization of the field [lying in the (x, y) plane] would be described by similar equations with additional terms arising from the plasma inhomogeneity in the x direction, which are, however, not expected to lead to a markedly different behavior. The present formalism is well adapted to modeling the amplification of HOH pulses since they are linearly polarized. Equation (1) is self-consistently solved together with the equation describing the evolution of the time envelope of the atomic polarization density on the lasing transition,

$$\frac{\partial P_\pm}{\partial t} = -\gamma P_\pm - i\omega D E_\pm + \Gamma_\pm, \quad (2)$$

where γ is the dipole dephasing factor arising from elastic and inelastic collisions of the lasing ions with other particles in the plasma [15]; this parameter plays a crucial role in the phenomena under study since it bears on the gain curve (value at line center and frequency width) and on the temporal dynamics of the polarization density, as evidenced by Eq. (2). D is the reduced, nondimensional population inversion density between the upper and lower x-ray lasing levels,

$$D = \frac{d^2}{\hbar\omega}(\rho_u - \rho_l), \quad (3)$$

where d is the absolute value of the nondiagonal matrix element of the dipole operator, ρ_u (ρ_l) is the dimensional population of the upper (respectively, lower) level. If the atomic relaxation rates are strong enough, the atomic populations can be described by the approximation of a quasistationary state, so that D can be written

$$D = \frac{\gamma}{8\pi\omega}\left(\frac{G_0\lambda}{\pi} + \frac{c}{I_{\mathrm{sat}}}\,\mathrm{Im}(P_- E_-^* + P_+ E_+^*)\right), \quad (4)$$

where G_0 is the small-signal gain at line center, λ is the XRL wavelength, and I_{sat} is the saturation intensity. The noise term $\Gamma_\pm$ in Eq. (2) accounts for spontaneous emission in the polarization considered. It must thus be noticed that the spontaneous radiation (and ASE) intensity in this model is only half the value that would be measured in experiments which do not discriminate between polarizations.

To perform detailed simulations we have upgraded COLAX in the following way. Local plasma conditions were determined by the TW angle and the EHYBRID time history of the plasma. EHYBRID provided us with the cell position, electron density, electron and ion temperatures, populations of the upper and lower x-ray lasing levels, small-signal gain, dipole dephasing factor, and the saturation intensity as functions of time and of the Lagrangian cell positions in the transverse (x) direction. By fixing plasma conditions along the transverse axis at a fixed y

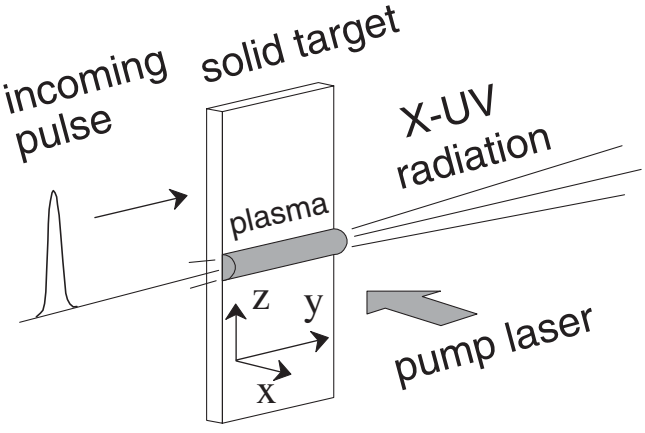

FIG. 1. Schematic diagram of a typical XRL setup for HOH amplification, with coordinate axes for numerical modeling.

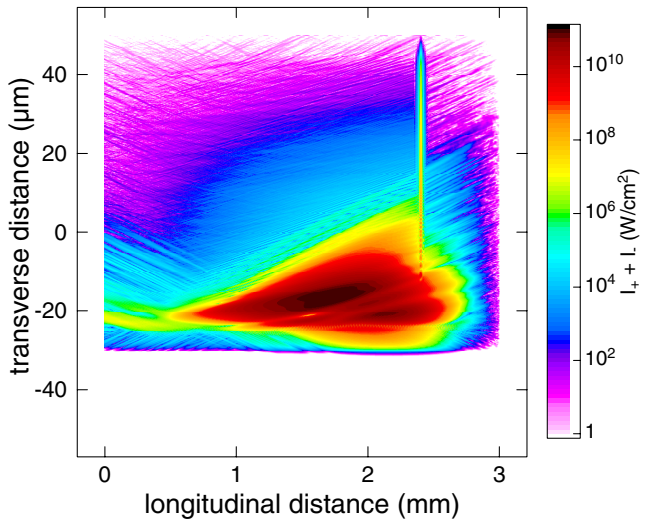

FIG. 2 (color online). A map of the total (forward + reverse) local XRL intensity at $t = 10$ ps inside the amplifying plasma. Notice the strongly different scales in the longitudinal and transverse directions. The narrow feature around $y = 2.4$ mm is the HOH pulse.

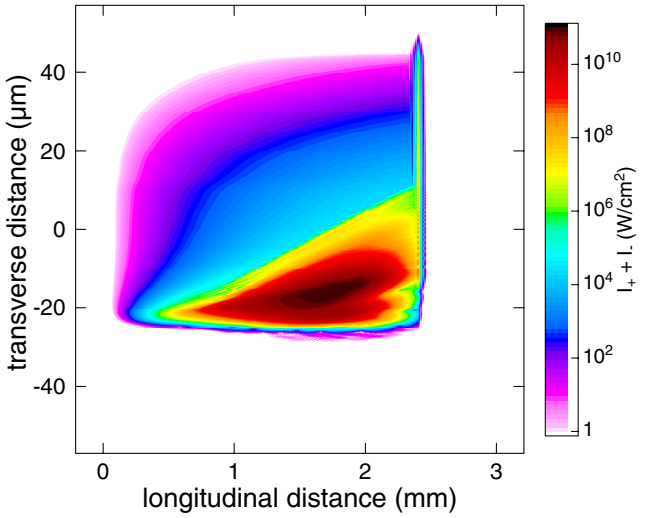

FIG. 3 (color online). A map of the local XRL intensity inside the amplifying plasma at $t = 10$ ps with spontaneous emission suppressed, showing only the HOH pulse and its wake.

coordinate, conditions at other y coordinates are calculated, using a space and time interpolation procedure, taking into account the time delay of the irradiation front of the traveling wave. The HOH pulse was taken into account through a modified time-dependent boundary condition for the electric field on the left ($y = 0$) boundary of the plasma.

Figure 2 shows a typical output from COLAX for a 3-mm-long plasma 10 ps after the start of the TW pumping stage, with parameter values as described above. This figure leads to the following conclusions. First, the HOH pulse, with peak intensity around 10^9 W/cm^2, is not appreciably amplified in itself. Instead, the HOH induces a long-lasting wake which is amplified to a high intensity (of order 10^{11} W/cm^2). The HOH wake is mixed with another feature which is attributed to the regular ASE signal. An inspection of the value of D obtained in the simulation shows that the equivalent small-signal gain at line center $G = 8\pi^2\omega D/\gamma\lambda$ is strongly saturated in the wake and ASE regions.

To clearly understand the nature of such an intensity distribution we ran COLAX including only the HOH pulse, setting spontaneous emission to zero. Results are shown in Fig. 3. One can see that the wake feature is essentially unchanged, and thus does not depend on the ASE. In Fig. 4, on the other hand, no HOH was injected, so that only spontaneous emission is amplified. In that case, as expected, only the ASE feature (propagating ahead of the HOH pulse in Fig. 2) is rendered.

Interpretations of experimental results heretofore published (e.g., Ref. [7]) implicitly rely on the notion of atomic susceptibility (see, e.g., [16]) which is obtained in the frame of the adiabatic hypothesis, wherein the left-hand side of Eq. (2) is set equal to $-i\delta\omega P_{\pm}$ where $\delta\omega$ is a frequency detuning of the applied signal with respect to the XRL transition frequency ω, and the applied signal amplitude is assumed constant in time. Running COLAX in the adiabatic approximation mode (which is an available option in the code) with a vanishing detuning (or in other words, for exact resonance with the XRL line), we obtained significantly different results. Figure 5 shows the intensity snapshot calculated using that model, to be compared with Fig. 2. One can see that, first, the short HOH pulse is much more amplified than in the time-dependent case. Second, the adiabatic approximation does not predict the existence of the long-lasting electric field wake. Such results, in contrast to the fully time-dependent results of Fig. 2, cannot explain the experimental data of Ref. [7], where amplification is observed mainly in the narrow spectral feature

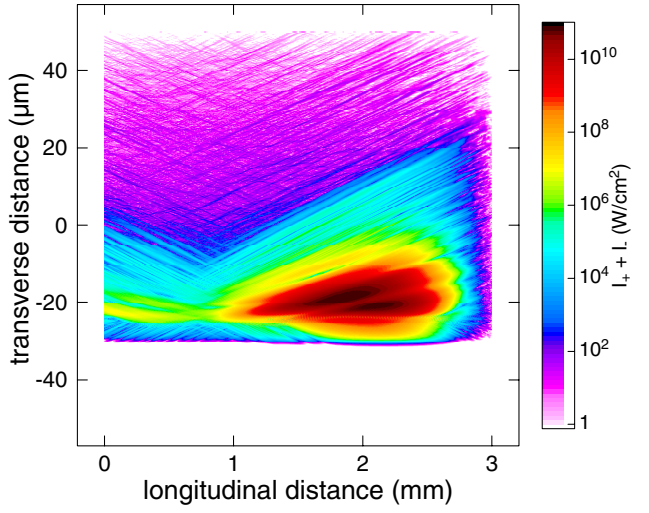

FIG. 4 (color online). A map of the local XRL intensity inside the amplifying plasma at $t = 10$ ps with no HOH pulse, showing only the ASE signal.

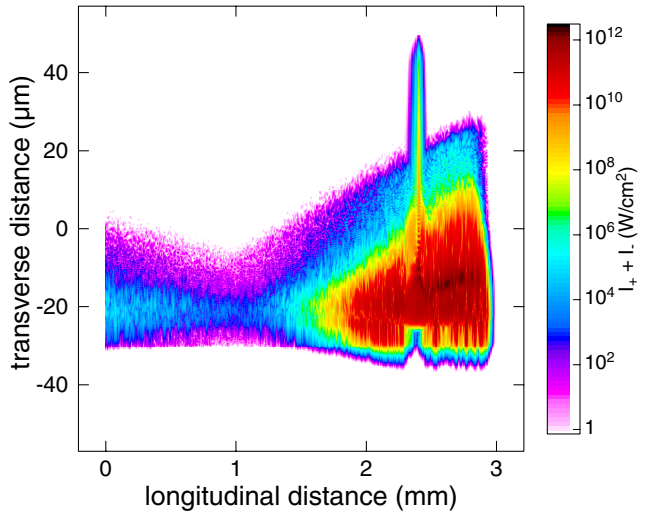

FIG. 5 (color online). A map of the local XRL intensity at $t = 10$ ps inside the amplifying plasma with an adiabatic calculation of the atomic polarization density.

arising from the XRL line, and not in the broad feature accounting for the HOH pulse.

We conclude that the amplification of short pulses is an intrinsically dynamic process which can be accounted for only through a fully time-dependent treatment of the atomic polarization density. This in turn allows us to correctly explain the narrow spectrum found in Ref. [7] for the amplified signal, allowed by its long duration since it takes the form of the wake seen in our results.

Let us emphasize that only a fully time-dependent calculation, as is performed in COLAX, can correctly account for the temporal evolution of the wave and associated polarization density, leading in turn to the correct spectral behavior. Radiation transfer methods cannot correctly account for the temporal dynamics of the system since they consider only the power density of the waves (i.e., the frequency-dependent specific intensity I_ν), discarding all spectral phase information. Some (possibly wrong) temporal behavior is then implicitly assumed in such calculations. In the case of the steady-state convective amplification of a constant incoming signal, the field is assumed [16] to be in the form of an incoherent superposition of random-phase Fourier modes with constant amplitude. In the usual informal generalization of that situation to the amplification of time-dependent pulses, the assumption is made that an incident wave train will be merely amplified during its propagation, otherwise retaining an essentially unchanged temporal profile. Clearly such an assumption is at fault in the present case, and cannot account for the specific time dynamics which leads to the wake seen in our simulations. As a consequence, radiation-transfer-like methods lead to erroneous results as illustrated in Fig. 5, namely, that the HOH pulse is strongly amplified while retaining its short duration, and that the maximum intensity is 20 times as large as in the correct time-dependent polarization case. This latter result can be related to the ray-tracing simulation presented in Ref. [9] which displays (in their Fig. 5) a computed outgoing intensity significantly larger than the experimentally recorded values, taking into account the given error bars.

In summary, the improved version of the COLAX code allows us to correctly interpret available experimental data on the amplification of HOH pulses in a XRL plasma, and to optimize the parameters of new experiments to be performed shortly, to inject the highest possible energy into the amplified signal. Specifically, our results emphasize an intrinsic difficulty on the way to truly "femtosecond" XRLs through the amplification of short HOH pulses, namely, the fact that the laser tends to operate over its natural time scale of order $1/\gamma$ rather than the incident pulse time scale. Thus, a relevant strategy to achieve shorter XRL pulses must involve a decrease of the natural laser time scale.

COLAX can also yield results pertaining to the coherence of the laser, which will be investigated and discussed in a more detailed paper. The development of the numerical modeling of those systems is going on. The next required step in that process is to relax the quasistationary state approximation used up to now [leading to an inversion density in the form of Eq. (4)] and perform instead a fully time-dependent treatment of the populations involved in gain generation. The role of inhomogeneous broadening of the XRL line should also be investigated.

*Corresponding author.
olivier.larroche@cea.fr

[1] V. Ayvazyan *et al.*, Eur. Phys. J. D **37**, 297 (2006).
[2] D. L. Matthews *et al.*, Phys. Rev. Lett. **54**, 110 (1985).
[3] *Proceedings of the 10th International Conference on X-Ray Lasers, 2006*, Springer Proceedings in Physics No. 115, edited by P. V. Nickles and K. A. Janulewicz (Springer, New York, 2007).
[4] K. Cassou *et al.*, Opt. Lett. **32**, 139 (2007).
[5] O. Guilbaud *et al.*, Europhys. Lett. **74**, 823 (2006).
[6] T. Ditmire *et al.*, Phys. Rev. A **51**, R4337 (1995).
[7] P. Zeitoun *et al.*, Nature (London) **431**, 426 (2004).
[8] T. Kawachi *et al.*, Proc. SPIE Int. Soc. Opt. Eng. **5919**, 59190L (2005).
[9] Y. Wang *et al.*, Phys. Rev. Lett. **97**, 123901 (2006).
[10] A. Klisnick *et al.*, J. Quant. Spectrosc. Radiat. Transfer **99**, 370 (2006).
[11] C. Chanteloup *et al.*, J. Opt. Soc. Am. B **17**, 151 (2000).
[12] G. J. Pert, J. Fluid Mech. **131**, 401 (1983).
[13] S. Kazamias *et al.*, Eur. Phys. J. D **21**, 353 (2002).
[14] O. Larroche *et al.*, Phys. Rev. A **62**, 043815 (2000).
[15] J. Dubau, C. Blancard, and M. Cornille, High Energy Density Phys. **3**, 76 (2007).
[16] A. Yariv, *Quantum Electronics* (Wiley, New York, 1989), 3rd ed.